PCCP

Accepted Manuscript

ROYAL SOCIETY OF CHEMISTRY

www.rsc.org/pccp

Journal Name

RSCPublishing

ARTICLE

Single-Molecule Spectroscopy and Femtosecond Transient Absorption Studies on Excitation Energy Transfer Process in ApcE(1-240) Dimer

Cite this: DOI: 10.1039/xoxxoooooox

Received ooth January 2012,
Accepted ooth January 2012

DOI: 10.1039/xoxxoooooox

www.rsc.org/

Saran Long,[a] Meng Zhou,[a] Kun Tang,[b] Xiao-Li Zeng,[b] Yingli Niu,[a] Qianjin Guo,[a] Kai-Hong Zhao[b,]* and Andong Xia[a,]*

ApcE(1-240) dimer with one intrinsic phycocyanobilin (PCB) chromophore in each monomer that is truncated from core-membrane linker (ApcE) of phycobilisomes (PBS) in *Nostoc* sp. PCC 7120, shows a sharp and significantly red-shifted absorption. Two explanations either conformation-dependent Förster resonance energy transfer (FRET) or the strong exciton coupling limit have been proposed for red-shifted absorption. This is a classic example of the special pair in the photosynthetic light harvesting proteins, but the mechanism of this interaction is still a matter of intense debate. We report the studies using single-molecule and transient absorption spectra on the interaction in the special pair of ApcE dimer. Our results demonstrate the presence of conformation-dependent FRET between the two PCB chromophores in ApcE dimer. The broad distributions of fluorescence intensities, lifetimes and polarization difference from single-molecule measurements reveal the heterogeneity of local protein-pigment environments in ApcE dimer, where the same molecular structures but different protein environments are the main reason for the two PCB chromophores with different spectral properties. The excitation energy transfer rate between the donor and the acceptor about $(110ps)^{-1}$ is determined from transient absorption measurements. The red-shifted absorption in ApcE dimer could result from more extending conformation, which shows another type of absorption redshift that does not depend on strong exciton coupling. The results here stress the importance of conformation-controlled spectral properties of the chemically identical chromophores, which could be a general feature to control energy/electron transfer, and widely exist in the light harvesting complexes.

Introduction

Phycobilisomes (PBS) found in cyanobacteria and red algae, contain various photosynthetic light harvesting biliproteins, such as phycoerythrins, C-phycocyanins (CPC) and allophycocyanins (APC), and they are assembled in rod-like structures with phycoerythrins at the outer ends of the rods, CPC in the middle, and APC in the center due to the organization of linkers including core-membrane linker (ApcE).[1-3] These proteins are open-chain tetrapyrrole-containing proteins in the PBS, providing the basis for the broad visible absorption spectrum. The strong coupling exciton models are often dealt with in multichromophore involvement in photosynthetic complexes. Of special interest is the APC trimer and ApcE dimer, which shows a significantly red-shifted absorption relative to CPC despite they all have the same phycocyanobilin (PCB) chromophores. X-ray diffraction studies on crystals of APC trimer shows (see Figure S1, ESI†)[4] that APC is a disc-like, trimeric protein with C_3-symmetry, which owns a diameter of approximately 11 nm, a thickness of roughly 3 nm and a central channel of 3.5 nm in diameter. There are two subunits (α84 and β84) in an APC monomer (In the following, the heterodimeric αβ protomer will be called a monomer and larger aggregates will be named according to the number of such monomers that they contain), and each subunit has a single open-chain tetrapyrrole chromophore, called phycocyanobilin (PCB). The distance between two adjacent α84 and β84 chromophores in the neighboring monomers within an APC trimer is 2.1 nm, whereas the distance between two chromophores within the same monomer is about 5.0 nm. The absorption spectrum of the APC trimer is considerably different from that of the monomer where only a broad and structureless absorption spectrum with a maximum at 615 nm is seen in APC monomer, whereas an unusual absorption maximum at 650 nm is observed upon going from monomers to trimers. Anyway, the mechanism for this spectral change is not clear until now in the past two decades, even after various spectroscopic researches including the steady-state absorption, circular dichroism, single-molecule and transient spectral measurements.[5-12] This is a classic example of the special

interaction of chromophore pair in the photosynthetic light harvesting proteins. Two explanations either Förster resonance energy transfer (FRET) or the strong exciton coupling limit have been proposed for the sharp and red-shifted absorption as introduced in ref. 2. One is so-called the chromophore conformation-dependent donor-acceptor model, where the particular local protein environment upon going from monomers to trimers produces certain chromophores with the 650 nm maximum, then energy is transferred from the 620-nm band to the 650-nm one by FRET.[5,7,11-13] Another one is the strong exciton model that the strong dipole-dipole interaction results in a split of the visible absorption spectrum in upper (620 nm) and lower (650 nm) exciton bands, where the 650-nm band is sharp, a characteristic of some exciton bands, and the energy transfer between two excitonic states occurs by internal conversion with time constant less than 100 fs.[6,8-10,14-17] Furthermore, it is known that FRET also occurred among the different strongly coupled pairs within APC trimer.[2] The fact that the APC trimer has both strong and weak couplings in the multichromophore system makes it very complicated to identify the mechanism of the complicated interactions among various PCB chromophores. For example, two reports have examined APC trimer using single-molecule spectroscopy, one group got three photobleaching steps of single APC trimer;[10] and the other obtained six distinct photobleaching steps of single APC trimer.[11] Moreover, femtosecond studies on APC trimer obtained results that supported the idea of FRET;[7] whereas some other femtosecond studies claimed the possible strong-coupling limit occurred in APC trimer.[6,8,9,16,17] Consequently, a simple model system seems to be required with less amount of chromophores but resembling the spectral properties of the unusual interaction in a pair of APC trimers through protein expression and reconstitution.[18,19]

Recently, a C-terminally truncated fragment ApcE(1-240) dimer containing the PCB chromophore binding at cysteine-195 was assembled in *Escherichia coli* through protein expression and reconstitution.[18,20] The truncated ApcE(1-240) is dimeric and each monomer contains one chromophore. It has an intense, red-shifted absorption at 660 nm of ApcE(1-240) dimer, similar to the red-shift features of the native APC trimer, demonstrating that the dimerization motif and the capacity to extremely red-shift the PCB chromophore are all contained in the ApcE(1-240).[18] The spectral tuning is very important for efficient energy transfer. Since the crystal structure of ApcE dimer is unknown until now, the simple dimeric ApcE(1-240) with the unique red-shifted absorption like APC trimer makes it particularly suitable for identifying the mechanism of the unusual interaction and energy transfer process between the interacted chromophores. For this purpose, steady state spectroscopy, single-molecule and femtosecond transient absorption measurements have been performed on the ApcE(1-240) dimer. Therefore, the red-shifted absorption in ApcE dimer could result from more extending conformation, which shows another type of absorption redshift that does not depend on strong exciton coupling. The results presented here stress the importance of the chromophore conformation and the heterogeneity of proteins in determining the spectral red-shift and directional energy transfer, which could be a general feature, and widely exist in the light harvesting antenna complexes.

Experimental Methods

Materials

ApcE(1-240) is assembled in *Escherichia coli* and purified via Ni^{2+} affinity chromatography according to the same procedures as the reported.[19] The plasmid pET-apcE(1-240) expressing the N-terminal fragment (amino acid between 1-240) of ApcE from *Nostoc* sp. PCC 7120 containing the chromophore domain, in which cysteine-195 can be attached to PCB,[18] and plasmid pACYC-ho1-pcyA expressing heme oxygenase HO1 and PCB reductase PcyA[21] were used. The purified ApcE(1-240) was kept in potassium phosphate buffer (20 mM KPB, 0.5 M NaCl, pH 7.2). Due to its low solubility, ApcE(1-240) in the buffer is saturated, and clarified via a short centrifugation before spectral measurements.

Steady-State Spectroscopy

The absorption spectrum was recorded by a UV-vis spectrophotometer (U-3010, Hitachi, Japan), and the fluorescence spectrum was measured with a fluorescence spectrophotometer (F-4600, Hitachi, Japan).

Single-Molecule Spectroscopy

Thin films of water-soluble poly (vinyl alcohol) (PVA) matrix doped with ApcE(1-240) dimer for single-molecule measurements were prepared by spin-coating of ~10^{-10} M solutions in KPB buffer onto a thoroughly cleaned glass coverslip. This yielded a 100-200 nm thick polymer film.

Single-molecule measurements were performed with a time-resolved confocal fluorescence microscope (MicroTime200, PicoQuant, Germany),[22] in which individual molecule fluorescence images were recorded by raster scanning the sample through the excitation light being focused by means of a linearized x-y-z piezo scanner. Through imaging, single 10μm×10μm sample areas of 10-15 molecules were obtained, and then individual molecules were positioned in the laser focus to measure the fluctuations in intensity with time. A PC plug-in card (TimeHarp200, PicoQuant, Germany) allowing for time-correlated single photon counting (TCSPC) with time-tagged time-resolved (TTTR) mode was used to register the detected photon from a single-photon avalanche diode (SPAD) (SPCM-AQR-13, PerkinElmer, USA). The TTTR mode allows the simultaneous registration of a detected photon on two independent time scales: the TCSPC time (~40 ps/channel) relative to the excitation laser pulse and the macroscopic arrival time (with 100 ns time resolution) on a continuous time axis relative to the start of the measurement. For excitation, a pulsed laser diode (635 nm, 100 ps, 40 MHz) (LDH-P-635, PicoQuant, Germany) was used. The collimated laser beam after a polarization-maintaining single-mode fiber was changed from linear to circular by a polarizer and a λ/4-plate and spectrally filtered by an excitation filter (D637/10, Chroma, USA) before being directed into the inverted microscope body (IX71, Olympus, Japan). A dichroic mirror (Q655LP, Chroma, USA) reflected the laser light into a high-aperture oil immersion objective (100×/1.40, PlanApo, Olympus, Japan). Single-molecule fluorescence was collected through the same objective and transmitted through the dichroic mirror. After passing one emission band-pass filter (HQ675/40, Chroma, USA), a tube lens (200 mm focal length) focused the fluorescence onto a 100 μm pinhole for confocal imaging. The fluorescence after this pinhole was refocused onto the active area of the SPAD. For polarization measurements, two single SPADs were used to collect the two orthogonal polarization components (s and p components) of the fluorescence split by a polarizing beamsplitter cube. The instrumental response

function (IRF) of the entire system was measured to be about 400 ps (FWHM). Single-molecule data were analyzed by the on-line MicroTime200 software (SymPhoTime v5.2.4, PicoQuant, Germany). All single-molecule measurements were performed in an N_2 atmosphere allowing for both a better observation of fluorescence and a large increase in the photochemical stability of ApcE(1-240) dimer molecules.

Femtosecond Transient Absorption Measurements

The femtosecond transient absorption measurements with ~90 fs time-resolution were measured using homemade femtosecond broadband pump-probe setup.[23,24] Briefly, a regeneratively amplified Ti:sapphire laser (Coherent Legend Elite) produced 40 fs, 1 mJ pulses at a 500 Hz repetition rate with a spectrum centered at 800 nm and a bandwidth of 40 nm (FWHM). The output from the amplifier was split by a 90/10 beamsplitter into pump and probe beams. A portion of the 800 nm fundamental light was used to pump a collinear optical parametric amplifier of white-light continuum (TOPAS-C, Light Conversion, Lithuania) to provide the excitation pulse at 605 nm with pulse width about 90 fs. About 80 nJ/pulse at 605 nm used for pumping was focused into the sample with a 120 μm spot. The probe beam at 800 nm was sent to a variable optical delay line, which comprises of a retro-reflector mirror on a computer controlled precision translation stage with a temporal resolution of 1 fs. The probe beam was then focused on a 2-mm-thick water cell to generate a white light continuum (WLC). The WLC provided a usable probe source between 420 and 780 nm selected by a suitable bandpass filter. The WLC was then split into two beams by using a broadband 50/50 beamsplitter for reference and signal beams. The signal beam was focused into a flow cell with 1 mm path length and spatially and temporally overlapped with the pump beam at 605 nm in the liquid sample, while the reference beam passed through the unexcited volume of the sample. Both reference and signal beams after the sample were focused into optical fibers of a dual-channel spectrometer (Avantes AvaSpec-2048-2-USB2) triggered from the same synchronized optical chopper driver at 500 Hz. A synchronized optical chopper (New Focus Model 3501) with a frequency of 250 Hz was inserted into the pump beam path in order to record probe spectra that were classified as pumped and not-pumped spectra, thereby reducing background effects. Every spectrum was recorded 200 times and the average spectrum was used in further data processing. Using the two-beam method, a few algorithms of data acquisition can be applied with the most common being a relative normalization of the spectral intensity of the signal to the spectral intensity of the reference. For each pump pulse, spectral intensities of the signal and the reference without any excitation in the sample, I_{signal}^{off} and I_{ref}^{off}, respectively, and I_{signal}^{on} and I_{ref}^{on} in the presence of the pump, were measured. Then the ΔOD of the transient absorption (for a given time delay) can be calculated from the following formula:

$$\Delta OD(t,\lambda) = -\log\left(\frac{I_{signal}^{on}(t,\lambda)}{I_{signal}^{off}(t,\lambda)} \times \frac{I_{ref}^{off}(t,\lambda)}{I_{ref}^{on}(t,\lambda)}\right) \quad (1)$$

A wavelength-dependent time-zero correction was performed to account for the group velocity dispersion of the probe beam.

The polarizations of pump and probe beams were set to 54.7º (magic angle), 0º ($I_{\parallel}$) and 90º ($I_{\perp}$), respectively for femtosecond time-resolved transient isotropy and anisotropy absorption measurements by rotating a 1/2 waveplate in pump beam, where $I_{\parallel}$ and $I_{\perp}$ represent transient absorption signals with the polarization of the pump and probe pulses being mutually parallel and perpendicular, respectively. For the time resolved transient absorption anisotropy measurement, both $I_{\parallel}$ and $I_{\perp}$ signals were calculated according to the following equation based on the tail matching correction:

$$r(t) = \frac{I_{\parallel}(t) - I_{\perp}(t)}{I_{\parallel}(t) + 2I_{\perp}(t)} \quad (2)$$

For the pump-probe measurements, the concentration of ApcE(1-240) dimer in KPB buffer was adjusted to an absorbance of 0.15 OD at 605 nm in a 1 mm path length quartz cuvette. No photodegradation was observed after femtosecond transient absorption measurements.

Results and Discussion

Steady-State Spectroscopy

Figure 1 shows the steady-state absorption, fluorescence and fluorescence excitation anisotropy spectra of ApcE(1-240) dimer in KPB buffer. The ApcE (1-240) dimer has a maximal absorption peak around 660 nm with a shoulder around 620 nm, while the emission peak is around 675 nm with a 'mirror symmetry' relationship to the absorption peak of 660 nm. The shapes of both the absorption and fluorescence spectra of ApcE(1-240) dimer are reminiscent of trimeric allophycocyanin-linker complexes.[18] To identify the interaction between the two chromophores in ApcE dimer, the fluorescence excitation anisotropy was measured in a PVA film, in order to avoid a rotation of molecules between excitation and fluorescence, while the absorption and fluorescence spectra have no changes after doping ApcE(1-240) dimer into PVA film. Fluorescence excitation anisotropy spectrum provided us a measuring result of the angle between the absorption and emission transition dipole moments of interacted chromophores. The anisotropy spectrum of ApcE(1-240) dimer shows a typical FRET feature as shown in Figure 1, where the anisotropy value is close to the theoretical maximum of 0.4 in the red region of 650-690 nm, but lower about 0.3 in the blue region of 580-630 nm. Thus, the exciton coupling model could be ruled out since exciton coupling leads to flat and lower anisotropy value (0.1) over all the spectral region.[25] Since the depolarization of the emission through rotational diffusion of molecules itself is suppressed in the PVA film, an intermolecular excitation energy transfer from donor to acceptor is involved in explaining the observed depolarization for the ApcE(1-240) dimer in the blue region of 580-630 nm, indicating that the two PCB chromophores with the same molecular structures in ApcE dimer have different absorptions where one acts as donor with absorption in the blue region of 580-630 nm and another one acts as a acceptor with absorption in the red region of 650-690 nm. The same molecular structures of PCBs but different conformations resulted from different protein environments in ApcE(1-240) dimer is the main reason for two PCB chromophores with different spectral properties, where the more coplanar the conformation of PCB chromophore is, the larger conjugated and the more red-shifted spectra are.[13] Therefore, the angle between donor's absorption and acceptor's emission transition dipole moments can be approximately calculated using,[25,26]

$$r = \frac{2}{5}\left(\frac{3\cos^2\beta - 1}{2}\right) \quad (3)$$

where, β is the displacement angle between the absorption and emission dipole moments. By taking r = 0.3, the relative angle between the transition dipole moments of donor chromophore (with absorption in the region of 580-630 nm) and acceptor chromophore (with fluorescence around 660-690 nm) is obtained as ~24º (or 156º), which is similar to the angle between transition dipole moments between adjacent α84 and β84 chromophores in APC trimer.[4,6,7]

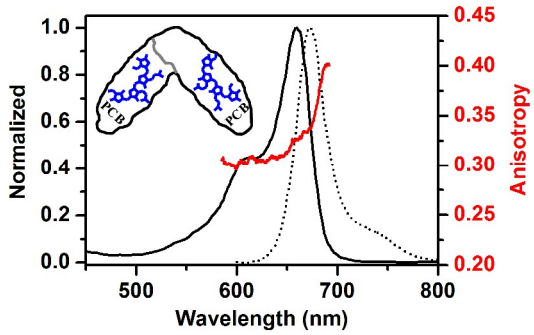

Figure 1. Normalized steady-state absorption (solid line), fluorescence (dotted line) and fluorescence excitation anisotropy (red line) spectra of ApcE(1-240) dimer in KPB buffer. The fluorescence excitation anisotropy spectrum was measured with the fluorescence at 710 nm. *Inset* shows the proposed model of ApcE dimer.

Single-Molecule Spectroscopy

Single-molecule spectroscopy has proven to be a powerful technique to identify the interaction mechanism between two interacting chromophores,[22,27-30] in which, the fluorescence time traces, simultaneously with the fluorescence lifetime and polarization from single dimers embedded in a PVA polymer matrix are measured. By comparing the spectral properties of the first-step and the second-step from those single molecules with two-step fluorescence time traces, the weak-coupling energy transfer or the strong-coupling exciton interaction between two chromophores can be identified at the single-molecule level. It is generally accepted,[10,22,28,31,32] that the spectral properties of first-step time-traces are from the dimeric interaction, and the emission is from interacting dimer units, which is described as two independent emitters due to the weak electronic coupling or a cooperative spontaneous emission (superradiance) from the two coupled emitters due to the strong electronic coupling, respectively; the second-step level was ascribed to the emission from one of the chromophore units in the dimer, while the other chromophore was photobleached. For those single dimers containing two coupled chromophores, the superradiance coherence factor L_S (L_S = $k_{dimer}/k_{monomer}$) should be a useful indicator, directly reflecting the interplay between intermolecular coupling strength, where the k_{dimer} and $k_{monomer}$ are the radiative rates of dimer and monomer from the first- and second-step time traces, respectively.

Thin films of water-soluble PVA matrix doped with ApcE(1-240) dimer for single-molecule measurements were prepared by spin-coating of 10^{-10} M ApcE(1-240) dimer solutions onto cleaned coverslips. Fluorescence intensities, lifetimes and polarization of single ApcE(1-240) dimers were measured simultaneously as a function of time. We focus our analysis on the two-step photobleaching molecules (63% ApcE dimer molecules show sequential one-by-one photobleaching, whereas the others show one-step photobleaching behavior), since they can provide important insight into the interchromophore coupling.[22,28,31] One-step photobleaching of ApcE(1-240) dimer result from the simultaneous photobleaching of the two chromophores or a dark state (radical or trap, etc) after the direct interaction of two chromophores upon excitation which quenches the residual chromophore emission.

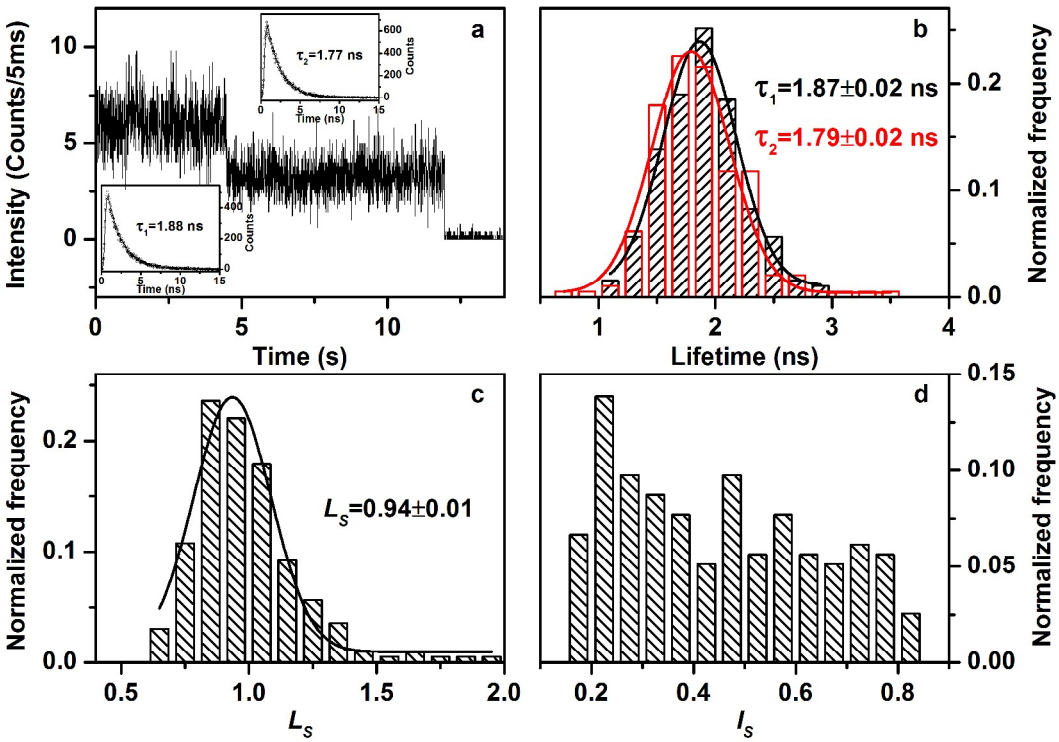

Figure 2. Single-molecule fluorescence behaviors of two-step photobleaching ApcE(1-240) dimer embedded in a PVA matrix. (a) Representative two-step fluorescence intensity time-traces with an integration time of 5 ms/bin. Single-exponential fluorescence decays of the first- and the second- steps are presented in *Insets*. (b) Normalized histograms of fluorescence lifetimes for the first-step (black) and the second-step (red) of 195 individual two-step bleaching molecules, and (c) Normalized distribution of superradiance coherence factor L_S for the same 195 molecules. Each histogram is fitted with a Gaussian distribution. (d) Normalized histogram of intensity-ratio I_S for the same set of molecules.

The typical fluorescence intensity time traces of single ApcE(1-240) dimers are shown in Figure 2a, and the corresponding fluorescence lifetimes are indicated at each intensity level. The two-step fluorescence time traces indicate that there are two successive excited-state processes in accordance with the number of the PCB chromophores in ApcE(1-240) dimer as is generally observed in most dimeric aggregates.[10,22,28,31,32]

We analyzed the single-molecule properties of 195 molecules with two-step behaviors. The lifetimes were obtained by maximum likelihood estimation (MLE) fitting with a single exponential model at each intensity level.[33] The histograms of the fluorescence lifetimes of the two-step behaviors are displayed in Figure 2b. From the Gaussian fits to the histograms, it is found for those single dimers with two-step behaviors that fluorescence lifetimes of the first-step is centered around 1.87 ns, and that of the second-step is around 1.79 ns, corresponding to the lifetimes of the ApcE(1-240) dimer and monomer, respectively. Both the average lifetimes from the first- and the second-step time traces are slightly longer than the ensemble fluorescence lifetime (1.5 ns) of ApcE(1-240) dimer. Likely, this is caused by the different environments: in the single-molecule measurements, the ApcE(1-240) dimer was embedded in a rigid PVA film and under N_2, while the ensemble lifetime was determined in buffer. The ratio L_S of the lifetimes of the second- and the first- intensity steps directly yields the superradiance coherence size of single dimers over the entire duration of the excited-state relaxation.[22,27,28,30,34] Figure 2c shows the L_S histogram from the 195 individual two-step bleaching ApcE(1-240) dimers. As illustrated by the distribution of L_S values centered at 0.94, the coupling strength between the two PCB chromophores in the ApcE(1-240) dimer is not strong enough to show the superradiance effect. No significant change in the fluorescence lifetime occurred with sequential photobleaching, indicating no (or weak) coupling between the two PCB chromophores within the ApcE(1-240) dimer.[22,30,35] The value of 0.94 is slightly smaller than 1.0, indicating a weak-coupling dimer. The same molecular structures of PCBs but different protein environments in the dimer is the reason for two PCB chromophores to have slightly different lifetimes within the first and second steps.[18] The observed broad distributions of intensities and lifetimes at single-molecule level result from the heterogeneity of local protein-pigment environments in ApcE(1-240) dimers. Thus, the single-molecule measurements suggest that the excitation energy transfer process in the ApcE(1-240) dimer is typically governed by chromophore conformation-controlled FRET mechanism.

The histogram of intensity-ratio I_S (the ratio of the second- and the first- step intensities) for the same set of molecules shows a broad distribution, as displayed in Figure 2d. Besides the 3D spatial distribution of the direction of the ApcE(1-240) dimer in a PVA film, this broad distribution results from the same molecular structures of PCBs, but different protein environments of two chromophores in the dimer, which could be evidenced from the changes in polarization of the second and first steps of two-step bleaching molecules.

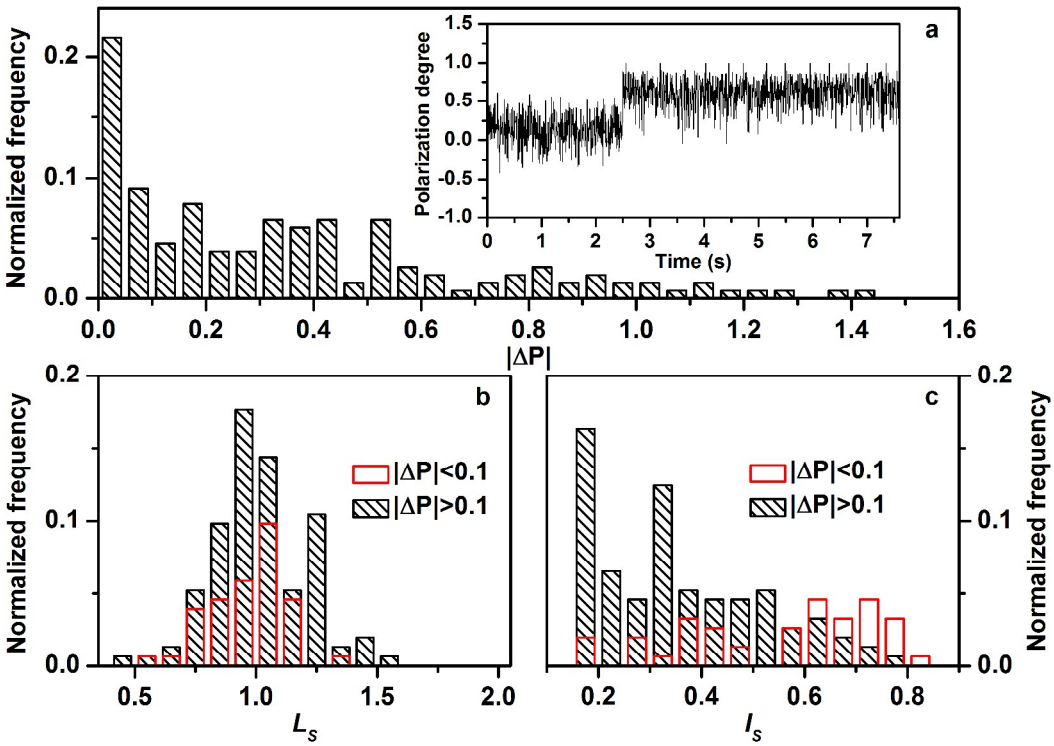

Figure 3. Distribution of |ΔP| and correlations of L_S and I_S with |ΔP| values. (a) Normalized histogram of the differences in polarization (|ΔP|) for 153 single molecules, showing two-step photobleaching. *Inset* shows representative time-traces of the polarization (5ms/bin) of a single ApcE dimer for first- and second-steps. (b, c) Histograms of superradiance coherence factor L_S and intensity-ratio I_S with |ΔP| < 0.1 and |ΔP| > 0.1 for the same 153 molecules.

The polarization P of single-molecule fluorescence was calculated for each intensity level according to $P = (I_P - I_S)/(I_P + I_S)$, and the difference between P_2 and P_1 values of the second- and first-steps was determined for every two-step bleaching molecules, which is directly related to the change in the orientation of the transition dipole moment of the emitting chromophore.[36,37] The histogram of the absolute values of this difference ($|\Delta P| = |P_2 - P_1|$) from 153 two-step bleaching single molecules is plotted in Figure 3a, presenting a broad distribution with values ranging from 0 up to 1.42. Since the energy transfer occurs from the donor to the acceptor in the ApcE(1-240) dimer, the acceptor could generally be the emitting chromophore for the first step. For those molecules with small changes in P (|ΔP| < 0.1), as expected that the emitter is the same chromophore in the first and second steps. Nevertheless, those molecules displaying large values of |ΔP| (|ΔP| > 0.1), suggest a big change of transition dipole moment angle between the second- and first- steps emitters, indicating different chromophores emitting in the two steps. To investigate the correlations of superradiance coherence factor L_S and intensity-ratio I_S with |ΔP| values, the histograms of L_S and I_S related to the |ΔP| values have been categorized into two different components: superradiance coherence factor L_S and intensity-ratio I_S histograms for ApcE(1-240) dimers with small (|ΔP| < 0.1) and large (|ΔP| > 0.1) |ΔP| values, respectively. The resulting plots are displayed in Figure 3b, c. The L_S around 1.0 for those dimers with |ΔP| < 0.1, suggests that the typical FRET mechanism is dominated, where the acceptor chromophore is always emitting in the first and second steps. Meanwhile, as shown in Figure 3b, c, for those dimers with |ΔP| > 0.1, acceptor is photobleached and the fluorescence is from donor in the second step. The fact that most values of I_S are smaller than 0.5 and the L_S seems a little smaller than 1.0, results from the same molecular structures of PCBs but different protein environments, suggesting that the so-called heterogeneity of local protein-pigment environments could widely exist in the light harvesting antenna complexes. Anyway, the radical or some other non-emission dark state is also most likely formed after one of the two chromophores being photobleached, resulting in the intensity and lifetime fluctuations in the first and second steps. Similar fluctuation phenomena were also observed in previous single-molecule measurements of APC trimer.[10,11] Furthermore, the small amount of dimers with large |ΔP| around 0.7-1.4 might result from the possible isomerization of PCB chromophores in ApcE(1-240) dimers, since isomerization can lead to large changes in orientation of transient dipole moment of chromophore.[12,38-41]

Femtosecond Transient Absorption Measurements

To examine the excitation energy transfer processes in ApcE dimer, femtosecond transient absorption measurements were further performed on the ApcE(1-240) dimer in KPB buffer. Figure 4 shows the broadband femtosecond transient absorption spectra at different delay times of the ApcE(1-240) dimer following 605 nm, 90 fs excitation. According to the steady-state absorption and fluorescence spectra of the ApcE(1-240) dimer as shown in Figure 1, a broad overlap of the ground state bleaching (GSB) and stimulated emission (SE) can be seen as a negative band extending from 615 to 680 nm, accompanied by an additional negative SE band mainly in the region of 700-780 nm. This additional SE band belongs to the part of the main SE, which is observed because it is far from the intense GSB/SE region of ApcE(1-240) dimer in the region of 615-680 nm. As shown in Figure 4, there is one positive band as the excited state absorption (ESA) band mainly appearing at 430-575 nm

observed in the transient absorption spectra, and this ESA band probably extends to the GSB region in the spectral region of 585-620 nm, which cannot be seen because of scattering of the pump beam.

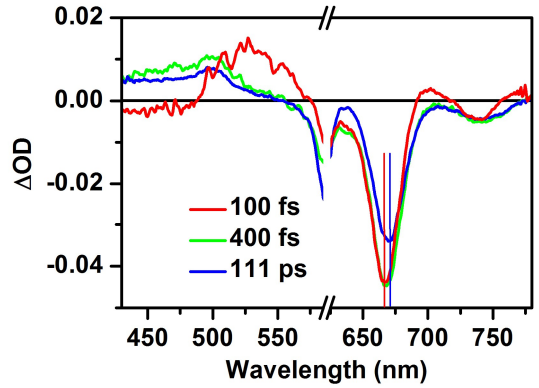

Figure 4. Transient absorption spectra at 100 fs, 400 fs and 111 ps delay times after 605 nm laser pulse excitation for the ApcE(1-240) dimer in KPB buffer. The two thin vertical lines represent the shift of the overlapped GSB and SE from donor and acceptor simultaneously, appearing at different delay times.

Together with the conclusion of the possible weak coupling limiting FRET mechanism for ApcE(1-240) dimer from the above-mentioned single-molecule experiments and steady-state measurements, a kinetic scheme shown in *Inset* of Figure 5a is proposed to extract the energy transfer rate, where the target global fitting procedure was then employed to extract the time-dependent concentrations of transient species and species associated difference spectra (SADS),[23,42-44] from the transient data as shown in Figure 4. Four components were required for an adequate fit of the transient data, while the applied target dynamic scheme (see *Inset* of Figure 5a) results in four lifetime values of 394 fs, 110 ps, 1.55 ns and 1.50 ns. The fitted time constants of ApcE(1-240) dimer are listed in Table 1. The corresponding SADS and the time-dependent concentrations of transient species are displayed in Figure 5a, b. In order to show the quality of fitting, kinetics at selected wavelengths of 500, 535, 655, 665, 675, 687, 700 and 740 nm are plotted together with a global fit of all the collected time traces (see Figure S3, ESI†). According to the decomposed absorption spectrum of ApcE(1-240) dimer as shown in Figure S2, the excitation at 605 nm is estimated to allow for a percentage (~30%) of direct excitation of acceptor chromophore, which shows a small population fraction of acceptor at the very initial time (see Figure 5b). As a comparison, we have also tried the target global fitting procedure based on the proposed kinetic model with the 100% of direction excitation of donor chromophore at 605 nm, similar results from target global fitting for SADS and time-dependent concentrations of transient species are obtained as shown in Figure S4 and S5 and Table S1 (ESI†).

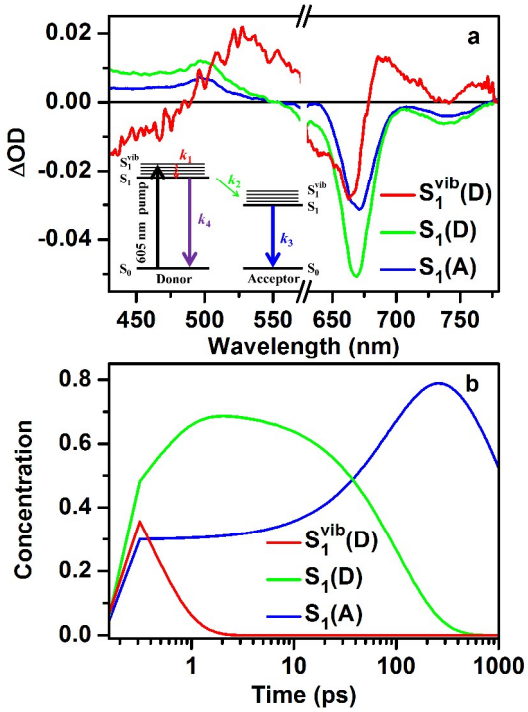

Figure 5. Global analysis of the transient absorption spectra based on the FRET model. (a) SADS obtained from target global fitting according to the FRET model described in *Inset*. (b) Time-dependent concentrations of the transient species. The fraction (70/30) of excitation for donor and acceptor at 605 nm is used during fitting.

Table 1. Rate constants estimated from global target analysis of ApcE(1-240) dimer.

k_1	k_2	k_3	k_4
$(394 \pm 30\ \text{fs})^{-1}$	$(110 \pm 10\ \text{ps})^{-1}$	$(1.55\ \text{ns})^{-1}$	$(1.50\ \text{ns})^{-1}$

The fraction (70/30) of excitation for donor and acceptor at 605 nm is used during fitting.

As shown in Figure 5, the first SADS (red line) corresponds to the excited state vibrational relaxation process with a time constant of 394 fs. A broad positive amplitude ESA from 500 to 580 nm, and a negative GSB around 630 nm and SE around 655 nm are clearly seen, indicating the donor is first excited to high vibrational states of the first excited state (S_1^{vib}). The second SADS (green line) rises in about 394 fs and has two decay times of 110 ps and ~1.50 ns, respectively, corresponding to the FRET from donor to acceptor, and the ground-state population recovery of donor. It is characterized by a pronounced excited-state absorption moved from 530 to 500 nm, and an overlapped GSB and SE bands from both donor and acceptor moved from 655 to 665 nm. The third SADS (blue line) shows a 110 ps rise, and then finally relaxes to the ground state of acceptor with a lifetime of ~1.55 ns, which is close to donor's lifetime.

Furthermore, the 110 ps excited state energy transfer process from donor to acceptor obtained from the transient isotropy absorption measurements is supported by the anisotropy pump-probe experiments. Figure 6 shows the transient anisotropy absorption decays of ApcE(1-240) dimer in pump-probe

experiments with the femtosecond pump wavelength at 605 nm and probe wavelengths at 645 nm (donor) and 675 nm (acceptor), respectively, where the 640 nm or 675 nm is corresponding to the broad overlapped GSB/SE of donor or acceptor chromophores in ApcE(1-240) dimer. All the transient anisotropy absorption decays in Figure 6 are well fitted with single-exponential function, and the fitted parameters are also presented. It is found that all the $r(0)$ at these probe wavelengths are all larger than 0.3 from a fitted asymptote of ~0.38 at 645 nm, and ~0.32 at 675 nm, which are near the theoretical maximum value of 0.4 at time zero. Upon excitation of donor at 605 nm, the time constant of the anisotropy decay at 645 nm (corresponding to high-energy donor's GSB/SE) is about 353 ps, and that at 675 nm (corresponding to low-energy acceptor's GSB/SE) is about 150 ps within experimental error. It is worth noting here that in the donor-acceptor FRET model, the anisotropy of donor probed at 645 nm after donor being excited at 605 nm, could be constant equal to 0.4 and without fast decay since the rotation of the big ApcE(1-240) dimer could be very slow, the 353 ps anisotropy decay at 645 nm results from the intense overlap of GSB/SE of donor with acceptor. Such intense overlap also simultaneously results in a slightly slower anisotropy decay time about 150 ps of acceptor compared to the 110 ps obtained from isotropy measurements while probe at 675 nm. The 150 ps time constant is very close to the 110 ps decay obtained from the isotropy results, which mainly corresponds to energy transfer from the high- to the low- energy chromophores by FRET in ApcE(1-240) dimer. The slightly large initial $r(0)$ around ~0.32 at the probe wavelength of 675 nm pumped at 605 nm indicates the small orientation angle (~21 degree) between donor and acceptor in ApcE dimer, which is in agreement with the steady-state fluorescence excitation anisotropy measurement as shown in Figure 1.

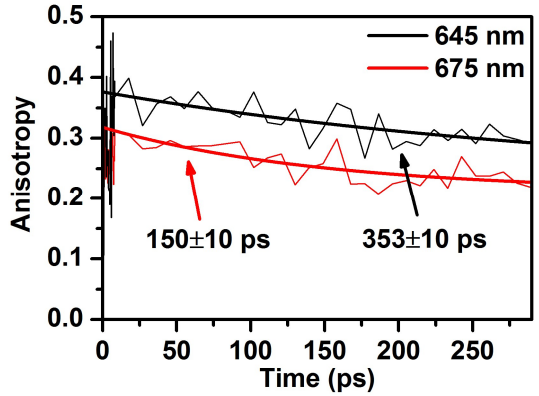

Figure 6. Time-resolved anisotropy of ApcE(1-240) dimer in KPB buffer at 645 nm and 675 nm corresponding to the SE of donor and acceptor, respectively. Well fitted with a single-exponential decay function having a 353 ps time constant from an initial anisotropy about 0.38 at 645 nm, and a 150 ps time constant with an intial anisotropy about 0.32 at 675 nm.

Anyway, small fraction of the denatured ApcE dimers that probably contributes to the observed slow anisotropy decay at 645 nm may exist with a cis-trans isomerization of the chromophore in ApcE(1-240) dimer.[12,38-40,45] This reaction can twist the chromophore and thus lead to a reorientation of the transition dipole. Although the photoisomerization in APC and CPC are not easily happened because of the rigid protein environments, very small amount of ApcE dimers may be denatured during sample preparation and measurements, thus the isomerization of the PCBs in denatured ApcE(1-240) dimers may possibly occur. This can also be seen from single-molecule polarization measurements as shown in Figure 3a, where a small distribution with large $|\Delta P|$ values around 0.7-1.4 might result from the possible isomerization of PCB chromophores in ApcE(1-240) dimer, since isomerization can lead to large change in orientation of transient dipole moment of chromophore.

Finally, it should be mentioned that we have also further attempted to fit the femtosecond time-resolved transient absorption data with strong interexciton level relaxation model (e.g. exciton coupling model) in ApcE(1-240) dimer, similar to what occurred in an exciton pair of chromophores within APC trimer and other light-harvesting proteins.[6,8,9,17,46] Anyway, no faster time constant (less than 200 fs) is obtained reasonably for the internal conversion from the upper- to the lower- exciton state as expected from strong coupling limit. Also, our femtosecond anisotropy decay shows that the $r(0)$ is larger than 0.3 at initial time after excitation, in which for strong exciton interaction of dimer, the $r(0)$ must be equal to 0.1.[47,48] This of course supports the donor-acceptor model occurred in ApcE(1-240) dimers, rather than the exciton coupling model.

Estimation of Distance

Since the x-ray structure of ApcE dimer is unknown until now, it is worthy to estimate the structural information from the obtained rate constants of ApcE(1-240) dimer based on the Förster theory.[49] The prediction of the Förster theory can be expressed in a convenient form:

$$k_{ET} = k_D \left(\frac{R_0}{R} \right)^6 \qquad (4)$$

where k_{ET} is the energy-transfer rate constant, R_0 is the Förster critical distance, R is the interchromophore distance, and k_D is the excited-state decay rate observed for the donor in the absence of the acceptor.

By considering the similarities between the properties and amino acid sequences of APC and ApcE(1-240) dimer, we assume similar geometry and spectral properties of the nearest neighbor PCB chromphores in ApcE(1-240) dimer and in APC trimers. In the latter, the APC monomeric unit is composed of an α and a β subunit, each of which binds a PCB chromophore via a thioether linkage to a cysteine residue at amino acid position 84.[4] The absorption spectrum of monomeric subunits of APC has a maximum near 615 nm which shifts to 650 nm upon trimer formation, which is similar to the absorption of ApcE(1-240) dimers. Thus, we can estimate the reasonable Förster critical distance R_0 between two PCB chromophores in ApcE(1-240) dimer according to the available energy transfer rate obtained from APC monomer and trimer.[6,7] Beck and Sauer obtained the 70 ps excitation transfer between the α84 and β84 PCB molecules within APC monomer in which two PCBs were separated by 5.0 nm distance.[6] Meanwhile, Sharkov and Gillbro obtained energy transfer time constant of 430 fs in APC trimer between two adjacent PCB chromophores with 2.1 nm separation.[7] Using the data $(70\ ps)^{-1}$ (k_{ET}) and $(1100\ ps)^{-1}$ (k_D) from ref. 6 as the excitation transfer rate and the excited-state decay rate of donor, respectively, for 5.0 nm separation between two PCB chromophores in APC monomer, we obtain $R_0 = 7.91$ nm; and by taking the excitation transfer rate $(430\ fs)^{-1}$ (k_{ET}) and the excited-state decay rate of donor $(1500\ ps)^{-1}$ (k_D) with 2.1 nm separation between two adjacent PCBs in APC

trimer from ref. 7, we obtain R_0 = 8.17 nm, very close to the R_0 = 7.91 nm in APC monomer. Therefore, according to equation (4), by taking the measured excitation transfer rate $(110\ ps)^{-1}$ (k_{ET}), the excited-state decay rate of donor $(1500\ ps)^{-1}$ (k_D), and estimated R_0 = 7.91~8.17 nm, we get R = 5.11~5.28 nm separation for the two PCB chromophores in ApcE(1-240) dimer. Such large separation further suggests the weak coupling FRET mechanism dominated in ApcE(1-240) dimer. It is worth mentioning here that, even at a large center-to-center distance around 5.11~5.28 nm in ApcE(1-240) dimer, there is almost perfect overlap between the emission of donor and the absorption of acceptor in ApcE(1-240) dimer, together with the well oriented mutually chromophores (about 24 degree), the radiationless resonance energy transfer from the donor can then be efficiently transferred to the acceptor in ApcE(1-240) dimer.

Conclusions

The ApcE(1-240) dimer which owns the similar spectral features as the APC trimer has been investigated in order to understand the mechanism of the unusual interaction and energy transfer between the two adjacent PCB chromophores in APC trimer and ApcE dimer by both single-molecule and transient absorption measurements. The single-molecule experiments suggest that the two chromophores are weakly coupled, where the same molecular structures of PCBs but different conformations resulted from different protein environments in ApcE(1-240) dimer is the main reason for two PCB chromophores with different spectral properties. The broad distributions of fluorescence intensities, lifetimes and |ΔP| values from single-molecule measurements could be a result of subtle changes to protein conformation, which is likely to reveal the heterogeneity of local protein-pigment environments in ApcE(1-240) dimer. Based on the Förster theory, by taking the energy transfer rate ~$(110\ ps)^{-1}$ determined from transient absorption measurements, the center-to-center distance about 5.2 nm between the two PCBs in ApcE(1-240) dimer is estimated. All the measurements in this work suggest that the red-shifted absorption of the ApcE(1-240) dimer is the result of conformational changes of chromophores, where in ApcE dimer there is no exciton coupling, in spite of the even larger red-shift than with APC trimer. The red-shifted absorption in ApcE dimer could result from more extending conformation, which shows another type of absorption redshift that does not depend on strong exciton coupling. The results presented here stress the importance of conformation-controlled spectral properties of the chemically identical chromophores with their individual microenvironments, which may be a general feature to control energy and electron transfer, and could widely exist in the light harvesting complexes.

Acknowledgements

We are grateful to Hugo Scheer (Munich University, Munich, Germany) for his critical reading and helpful suggestion. This work was supported by the 973 Program (2013CB834604), NSFCs (21173235, 91233107, 21127003, 21333012, 21373232 and 31110103912) and the Chinese Academy of Sciences (XDB12020200).

Notes and references

[a] Beijing National Laboratory for Molecular Sciences (BNLMS) and Key Laboratory of Photochemistry, Institute of Chemistry, Chinese Academy of Sciences, Beijing 100190, People's Republic of China. E-mail: andong@iccas.ac.cn.

[b] State Key Laboratory of Agricultural Microbiology, Huazhong Agricultural University, Wuhan 430070, People's Republic of China. E-mail: khzhao@163.com.

† Electronic Supplementary Information (ESI) available: The structure and absorption spectrum of APC trimer and additional information are included. See DOI: 10.1039/b000000x/

1 R. van Grondelle, *Biochim. Biophys. Acta*, 1985, **811**, 147-195.

2 R. MacColl, *Biochim. Biophys. Acta*, 2004, **1657**, 73-81.

3 A. N. Glazer, in *Advances in Molecular and Cell Biology*, ed. E. E. Bittar and J. Barber, Elsevier, Greenwich/London, 1994, vol. 10, pp. 119-149.

4 K. Brejc, R. Ficner, R. Huber and S. Steinbacher, *J. Mol. Biol.*, 1995, **249**, 424-440.

5 A. Murakami, M. Mimuro, K. Ohki and Y. Fujita, *J. Biochem.*, 1981, **89**, 79-86.

6 W. F. Beck and K. Sauer, *J. Phys. Chem.*, 1992, **96**, 4658-4666.

7 A. V. Sharkov, I. V. Kryukov, E. V. Khoroshilov, P. G. Kryukov, R. Fischer, H. Scheer and T. Gillbro, *Biochim. Biophys. Acta*, 1994, **1188**, 349-356.

8 M. D. Edington, R. E. Riter and W. F. Beck, *J. Phys. Chem.*, 1995, **99**, 15699-15704.

9 M. D. Edington, R. E. Riter and W. F. Beck, *J. Phys. Chem.*, 1996, **100**, 14206-14217.

10 L. Ying and X. S. Xie, *J. Phys. Chem. B*, 1998, **102**, 10399-10409.

11 D. Loos, M. Cotlet, F. De Schryver, S. Habuchi and J. Hofkens, *Biophys. J.*, 2004, **87**, 2598-2608.

12 R. H. Goldsmith and W. E. Moerner, *Nat. Chem.*, 2010, **2**, 179-186.

13 P.-P. Peng, L.-L. Dong, Y.-F. Sun, X.-L. Zeng, W.-L. Ding, H. Scheer, X. Yang and K.-H. Zhao, *Acta Crystallogr. Sect. D*, 2014, **70**, 2558-2569.

14 K. Csatorday, R. MacColl, V. Csizmadia, J. Grabowski and C. Bagyinka, *Biochemistry*, 1984, **23**, 6466-6470.

15 A. R. Holzwarth, E. Bittersmann, W. Reuter and W. Wehrmeyer, *Biophys. J.*, 1990, **57**, 133-145.

16 B. J. Homoelle, M. D. Edington, W. M. Diffey and W. F. Beck, *J. Phys. Chem. B*, 1998, **102**, 3044-3052.

17 J. M. Womick and A. M. Moran, *J. Phys. Chem. B*, 2009, **113**, 15747-15759.

18 K.-H. Zhao, P. Su, S. Böhm, B. Song, M. Zhou, C. Bubenzer and H. Scheer, *Biochim. Biophys. Acta*, 2005, **1706**, 81-87.

19 K. Tang, X.-L. Zeng, Y. Yang, Z.-B. Wang, X.-J. Wu, M. Zhou, D. Noy, H. Scheer and K.-H. Zhao, *Biochim. Biophys. Acta*, 2012, **1817**, 1030-1036.

20 A. Biswas, Y. M. Vasquez, T. M. Dragomani, M. L. Kronfel, S. R. Williams, R. M. Alvey, D. A. Bryant and W. M. Schluchter, *Appl. Environ. Microbiol.*, 2010, **76**, 2729-2739.

21 K.-H. Zhao, P. Su, J.-M. Tu, X. Wang, H. Liu, M. Plöscher, L. Eichacker, B. Yang, M. Zhou and H. Scheer, *Proc. Natl. Acad. Sci. U. S. A.*, 2007, **104**, 14300-14305.

22 D. Aumiler, S. Wang, X. Chen and A. Xia, *J. Am. Chem. Soc.*, 2009, **131**, 5742-5743.

23 M. Zhou, S. Vdović, S. Long, M. Zhu, L. Yan, Y. Wang, Y. Niu, X. Wang, Q. Guo, R. Jin and A. Xia, *J. Phys. Chem. A*, 2013, **117**, 10294-10303.

24 S. Vdović, Y. Wang, B. Li, M. Qiu, X. Wang, Q. Guo and A. Xia, *Phys. Chem. Chem. Phys.*, 2013, **15**, 20026-20036.

25 C. Sissa, A. Painelli, M. Blanchard-Desce and F. Terenziani, *J. Phys. Chem. B*, 2011, **115**, 7009-7020.
26 T. J. V. Prazeres, A. Fedorov, S. P. Barbosa, J. M. G. Martinho and M. N. Berberan-Santos, *J. Phys. Chem. A*, 2008, **112**, 5034-5039.
27 Y. Zhao, T. Meier, W. M. Zhang, V. Chernyak and S. Mukamel, *J. Phys. Chem. B*, 1999, **103**, 3954-3962.
28 M. Lippitz, C. G. Hübner, T. Christ, H. Eichner, P. Bordat, A. Herrmann, K. Müllen and T. Basché, *Phys. Rev. Lett.*, 2004, **92**, 103001.
29 J. Hernando, E. M. H. P. van Dijk, J. P. Hoogenboom, J.-J. García-López, D. N. Reinhoudt, M. Crego-Calama, M. F. García-Parajó and N. F. van Hulst, *Phys. Rev. Lett.*, 2006, **97**, 216403.
30 H. W. Bahng, M.-C. Yoon, J.-E. Lee, Y. Murase, T. Yoneda, H. Shinokubo, A. Osuka and D. Kim, *J. Phys. Chem. B*, 2012, **116**, 1244-1255.
31 M. Park, S. Cho, Z. S. Yoon, N. Aratani, A. Osuka and D. Kim, *J. Am. Chem. Soc.*, 2005, **127**, 15201-15206.
32 G. D. Scholes, K. P. Ghiggino, A. M. Oliver and M. N. Paddon-Row, *J. Am. Chem. Soc.*, 1993, **115**, 4345-4349.
33 M. Maus, M. Cotlet, J. Hofkens, T. Gensch, F. C. De Schryver, J. Schaffer and C. A. M. Seidel, *Anal. Chem.*, 2001, **73**, 2078-2086.
34 J. Yang, H. Yoo, N. Aratani, A. Osuka and D. Kim, *Angew. Chem., Int. Ed.*, 2009, **48**, 4323-4327.
35 M. Kasha, H. R. Rawls and M. A. El-Bayoumi, *Pure Appl. Chem.*, 1965, **11**, 371-392.
36 J. Hernando, M. van der Schaaf, E. M. H. P. van Dijk, M. Sauer, M. F. García-Parajó and N. F. van Hulst, *J. Phys. Chem. A*, 2003, **107**, 43-52.
37 T. Stangl, S. Bange, D. Schmitz, D. Würsch, S. Höger, J. Vogelsang and J. M. Lupton, *J. Am. Chem. Soc.*, 2013, **135**, 78-81.
38 M. Bischoff, G. Hermann, S. Rentsch, D. Strehlow, S. Winter and H. Chosrowjan, *J. Phys. Chem. B*, 2000, **104**, 1810-1816.
39 K. Heyne, J. Herbst, D. Stehlik, B. Esteban, T. Lamparter, J. Hughes and R. Diller, *Biophys. J.*, 2002, **82**, 1004-1016.
40 L. H. Freer, P. W. Kim, S. C. Corley, N. C. Rockwell, L. Zhao, A. J. Thibert, J. C. Lagarias and D. S. Larsen, *J. Phys. Chem. B*, 2012, **116**, 10571-10581.
41 N. C. Rockwell, L. Shang, S. S. Martin and J. C. Lagarias, *Proc. Natl. Acad. Sci. U. S. A.*, 2009, **106**, 6123-6127.
42 J. T. M. Kennis, D. S. Larsen, I. H. M. van Stokkum, M. Vengris, J. J. van Thor and R. van Grondelle, *Proc. Natl. Acad. Sci. U. S. A.*, 2004, **101**, 17988-17993.
43 L. J. G. W. van Wilderen, C. N. Lincoln and J. J. van Thor, *PLoS One*, 2011, **6**, e17373.
44 I. H. M. van Stokkum, D. S. Larsen and R. van Grondelle, *Biochim. Biophys. Acta*, 2004, **1657**, 82-104.
45 S. E. Braslavsky, A. R. Holzwarth and K. Schaffner, *Angew. Chem., Int. Ed.*, 1983, **22**, 656-674.
46 J. M. Womick and A. M. Moran, *J. Phys. Chem. B*, 2011, **115**, 1347-1356.
47 C. Galli, K. Wynne, S. M. LeCours, M. J. Therien and R. M. Hochstrasser, *Chem. Phys. Lett.*, 1993, **206**, 493-499.
48 K. Wynne and R. M. Hochstrasser, *Chem. Phys.*, 1993, **171**, 179-188.
49 T. Förster, *Ann. Phys.*, 1948, **437**, 55-75.

TOC Graphic

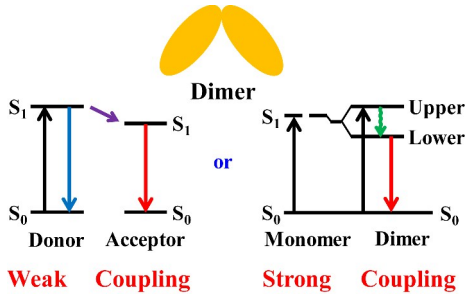

The red-shifted absorption of ApcE dimer results from extending chromophore conformation, that does not depend on strong exction coupling.